Mean-field theory for coarsening faceted surfaces

Scott A. Norris*
Department of Mathematics, Southern Methodist University, Dallas, Texas 75275, USA

Stephen J. Watson
School of Mathematics and Statistics, University of Glasgow, Glasgow, Scotland, G12 8QW, United Kingdom
(Received 12 October 2011; revised manuscript received 20 December 2011; published 29 February 2012)

A mean-field theory is developed for the scale-invariant length distributions observed during the coarsening of generic one-dimensional faceted surfaces. This theory closely follows the Lifshitz-Slyozov-Wagner theory of Ostwald ripening in two-phase systems, but the mechanism of coarsening in faceted surfaces requires the addition of convolution terms recalling work on particle coalescence, and induces an unexpected coupling between the convolution and the rate of facet loss. As a generic framework, the theory concisely illustrates how the universal processes of facet removal and neighbor merger are moderated by the system-specific mean-field velocity describing average rates of length change. For a simple, example facet dynamics associated with the directional solidification of a binary alloy, agreement between the predicted scaling state and that observed after direct numerical simulation of 40 000 000 facets is reasonable given the limiting assumption of noncorrelation between neighbors; relaxing this assumption is a clear path forward toward improved quantitative agreement with data in the future.

DOI: 10.1103/PhysRevE.85.021608 PACS number(s): 81.10.Aj, 05.20.Gg, 68.55.jm

I. INTRODUCTION

In many examples of faceted surface evolution, a *facet-velocity law* giving the normal velocity of each facet can be observed, assumed, or derived. Examples of such dynamic laws describe the growth of polycrystalline diamond films from the vapor [1,2], the evolution of faceted boundaries between two elastic solids [3], the evaporation-condensation mechanism of thermal annealing [4], and various solidification systems [5–9]. Such velocity laws are typically configurational, depending on surface properties of the facet such as area, perimeter, orientation, or position, and reduce the computational complexity of evolving a continuous surface to the level of a finite-dimensional system of ordinary differential equations. This theoretical simplification enables and invites large numerical simulations for the study of statistical behavior. This has been done frequently for one-dimensional surfaces [5–14], while less frequently for two-dimensional surfaces due to the necessity of handling complicated topological events [4,15–19]. Such inquiries reveal that many of the systems listed above exhibit coarsening—the continual vanishing of small facets and the increase in the average length of those that remain. Notably, these systems also display *dynamic scaling*, in which common geometric surface properties approach a constant statistical state, which is preserved even as the length scale increases.

The dynamic scaling behavior of coarsening faceted surfaces recalls the process of Ostwald ripening [20], in which small solid-phase grains in a liquid matrix dissolve, while larger grains accrete the resulting solute and grow in a scale-invariant way at late times. Indeed, it was observed some time ago that facets of alternating orientations on a one-dimensional surface are analogous to alternating phases of a separating two-phase alloy [21,22] and the Cahn-Hilliard equation [23], which models phase separation, has been used, in modified form, to describe several different kinds of faceted surface evolution [9,24,25]. More distantly related coarsening systems exhibiting dynamic scaling include coarsening cellular networks describing soap froths and polycrystalline films [26–30] and films growing via spiral defect [31]. In all of these cases, the system is characterized by a network of evolving boundaries that separate domains of possibly differing composition and exhibit coarsening and convergence toward scale-invariant steady states.

Because dynamic scaling pushes complex systems into a state that can be approximately characterized by just a few statistics, it is natural to seek simplified models that approximately mimic the resulting scaling laws and scaling functions. The canonical example of this approach is the celebrated theory of Lifshitz, Slyozov, and Wagner describing Ostwald ripening [32–34]. Generically, such an approach selects a distribution of some quantity and includes just enough of the total system behavior to specify the effective behavior of that quantity; for example, the original Lifshitz-Slyozov-Wagner (LSW) theory first identifies the average behavior of particles as a function of size and uses that result to identify a continuity equation describing distribution evolution. Ideas of this kind have been applied to several of the higher-order cellular systems introduced above: for soap froths [35,36], polycrystals [37], and spiral-growth films [31]. To the extent that such approaches mirror experimental data, they can yield valuable physical insight that cannot be gained by considering single particles or even by direct numerical simulation of larger ensembles. However, to date, no similar attempt has been made for evolving faceted interfaces, which is somewhat surprising given the wide variety of examples of purely faceted motion and past success in applying mean-field analyses to coarsening these systems.

In this work, therefore, we take a step in that direction by introducing a framework for describing the distribution of

*snorris@smu.edu

facet lengths in one-dimensional faceted surface evolution. Our approach closely resembles the LSW theory of Ostwald ripening, in that a number density $n(l,t)$, of facets of length l at time t, is transported by a known length-dependent effective velocity law. However, whereas vanishing drops in Ostwald ripening simply exit the system, each vanishing facet on a coarsening surface causes its two immediate neighbors to join together. Accounting for this process of merging requires the consideration of a convolution integral reminiscent of equations due to von Smoluchowski [38] and Schumann [39] describing coagulation (see also Ref. [40]). However, since the removal rate of small facets from the system necessarily sets the rate of the concomitant merger of those neighboring facets, a nonlocal coupling arises wherein the probability flux at the origin is found to weight the convolution integral. We therefore arrive at the resulting evolution equation for the probability distribution $\rho(l,t)$ of facets of length l at time t:

$$\frac{\partial \rho}{\partial t} + \frac{\partial}{\partial l}[\rho v] = -\rho(0,t)v(0,t)\int_0^l \rho(l-s,t)\rho(s,t)ds, \quad (1)$$

where the velocity $v(l,t)$ takes the special form

$$v(l,t) = \widehat{\mathcal{V}}[l, L(t)] \quad \text{for } L(t) \equiv \int_0^\infty l\rho(l,t)dl \quad (2)$$

for a derived and prescribed *mean-field velocity* law $\widehat{\mathcal{V}}(l,L)$, which encodes an effective rate of change of length for facets of length l purely in terms of that length l and the mean facet length L. The left-hand side of Eq. (1), in particular the appearance there of the mean-field velocity $\widehat{\mathcal{V}}(l,L)$, is precisely where our theory mimics the essential transport concept underlying the LSW theory. In contrast, the convolution on the right-hand side of Eq. (1) is strongly reminiscent of coagulation models. Finally, we note that the time-dependent function multiplying the convolution $(\rho * \rho)$,

$$\mathcal{R} = -\rho(0,t)v(0,t),$$

is a rate of probability flux at the origin, which encodes the link between facets shrinking to zero and the concomitant merger of the two neighboring facets.

II. EXAMPLE PROBLEM: FROM MODELING TO MORPHOMETRICS

A. Example coarsening dynamical system

During the directional solidification of a strongly anisotropic binary alloy, small-wavelength faceted surfaces develop. If the alloy is solidified above a critical velocity, a layer of supercooled liquid is created at the interface, which drives a coarsening instability governed by the facet dynamics [9]

$$\mathcal{V}_i = \mu \cos(\omega) h_i, \quad (3)$$

where $\mathcal{V}_i$ is the (instantaneous) normal velocity and h_i is the mean height of the ith facet. The constant μ is a mobility with units of $\sec^{-1}$; we may assume $\mu = 1$ without loss of generality, but will retain the constant to render units consistent. Finally, $(-1)^i\omega$ is the fixed facet angle (the Wulff angle); we assume throughout, for simplicity, that only two alternating facet orientations are present on the surface.

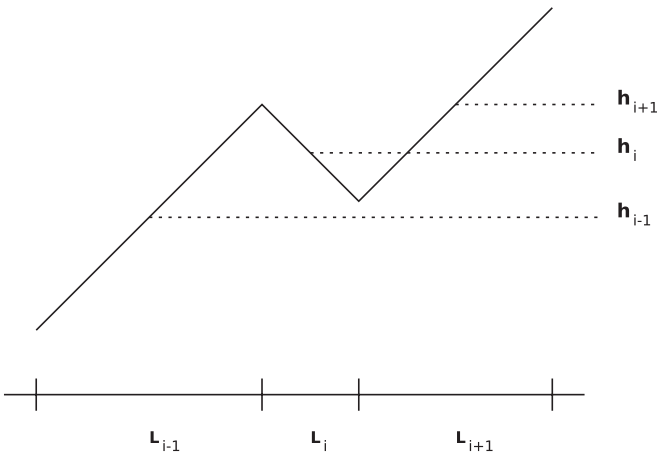

FIG. 1. Facet schematic: diagram illustrating a representative facet and its two neighbors. Here h_i denotes the mean height of the center facet and L_i denotes its width (length). The parameters are similar for the neighbors of the center facet.

Letting $l_i(t)$ denote the length of the ith facet at time t, we will now show that, between coarsening events, one can derive from Eq. (3) a dynamical system for these facet lengths. First, we note the general, kinematic relation

$$\frac{dl_i}{dt} = \frac{(-1)^i \mu}{\sin(2\omega)}(\mathcal{V}_{i+1} - \mathcal{V}_{i-1}); \quad (4)$$

the prefactor $(-1)^i$ reflects our convention that odd (even) facets have negative (positive) slopes. If we now use the facet velocity law (3) to specify the dynamics, we can convert this equation, via elementary geometry (see Fig. 1), to a dynamical system on facet lengths alone:

$$\frac{dl_i}{dt} = \frac{\mu}{4}(2l_i - l_{i+1} - l_{i-1}). \quad (5)$$

Thus, even though the normal velocity of a facet depends on its mean height and slope, the rate of change of its length does not.

Now the morphometric structure of the evolving coarsening faceted surface is encoded in an ordered facet-length ensemble, denoted $\mathcal{L}[t] : \mathbb{Z} \to (0,\infty)$, associated with the evolving interface; $\mathcal{L}[t](i) \equiv l_i(t)$. Since the dynamical system (5) results in lengths that tend to zero, resulting in the merging of the two neighboring facets (a coarsening event), we need to rewrite $\mathcal{L}[t]$ at such critical times. To see how, we again consider Fig. 1 and imagine that the jth facet F_j shrinks to length 0 at the critical time t^*. When this happens, this F_j obviously vanishes; however, in addition, the two neighbors of F_j, namely, F_{j-1} and F_{j+1}, also vanish as independent entities, to be replaced by a new facet with length equal to the sum of the lengths of its ancestors. A natural reindexing of the resultant faceted surface provides the update rule $\mathcal{L}[t_*^+]$,

$$\mathcal{L}[t_*^+](i) \equiv \begin{cases} \mathcal{L}[t_*^-](i+1), & i \leqslant j-2 \\ \mathcal{L}[t_*^-](j-1) + \mathcal{L}[t_*^-](j+1), & i = j \\ \mathcal{L}[t_*^-](i-1), & i \geqslant j+2. \end{cases} \quad (6)$$

Taken together, Eqs. (5) and (6) constitute a coarsening dynamical system (CDS), which is the object of our further study.

B. Numerical simulation and morphological statistics

For three different initial length distributions, random faceted surfaces containing 1 000 000 facets were constructed by generating two sets of numbers obeying that distribution and scaled to have equal sums; these random lengths were then interleaved to generate a periodic faceted surface. The initial empirical distributions of facet lengths $\varrho(l)$ were

$$\begin{aligned} \varrho_{0,\mathrm{comp}}(l) &= \frac{10}{18}\chi_{(1/10,19/10)}, \\ \varrho_{0,\mathrm{exp}}(l) &= \exp(-l), \\ \varrho_{0,\mathrm{poly}}(l) &= \frac{2}{(1+l)^3}. \end{aligned} \tag{7}$$

Hence we have explored initial distributions of facet lengths with compact support, exponential decay, and polynomial decay.

Figure 2(a) depicts a representative local patch of surface evolving under the CDS (5) and (6). There the locations of facet boundaries (corners) are plotted over time and we see many instances of the binary coarsening described by the update rule (6). As the system continues to evolve, all three initial conditions [Fig. 2(b)] begin to coarsen exponentially, with the average facet length $L(t) \propto e^{1.8t}$ at late times [Fig. 2(c)]. The arrival at this rate indicates the attainment of the *scaling state*, in which the associated empirical probability distribution $\varrho(l,t)$, of facet lengths l at time t, is observed to approach a universal scale-invariant form

$$\varrho(l,t) \xrightarrow{t\to+\infty} \frac{1}{L(t)}\mathfrak{P}\left(\frac{l}{L(t)}\right), \tag{8}$$

which is illustrated in Fig. 2(d).

III. MEAN-FIELD THEORY FOR BINARY-COARSENING FACETED SURFACES

We now turn to a theoretical study of the evolving facet ensemble associated with the CDS. Our focus is the formulation of a general theory that sheds light on the empirical probability distribution $\varrho(l,t)$. Inspired by the LSW theory, our aim is to formulate an approximation for ϱ by rationally constructing a mass-transport evolution equation for a theoretical probability function $\rho(l,t)$, supplemented by sinks or sources that simultaneously and properly account for the appropriate coarsening mechanism of the original CDS. Our closed theory emerges from a number of mean-field approximations of the underlying facet ensemble; such approximations are often referred to as *mean-field hypotheses*.

A. Preliminaries

We begin by introducing a number of quantities derived from $\rho(l,t)$ that are specific to coarsening systems. First, as small facets shrink to zero and are removed from the system, the average length $L(t)$ of the remaining facets increases. This monotonically increasing quantity is simply the first moment of ρ:

$$L(t) \equiv \int_0^\infty l\rho(l,t)dl.$$

Second, we define the number density $n(l,t)$ by

$$n(l,t) \equiv \left(\frac{L_0}{L(t)}\right)\rho(l,t), \tag{9}$$

where both L_0 and $L(t)$ have units of length; hence $n(l,t)$ and $\rho(l,t)$ have the same units of probability per unit length. [For convenience, we define $L_0 \equiv 1$ so that $n(l,t)$ describe number density per unit interface length of surface; however, we retain the symbol L_0 so that all equations retain consistent units.] Note that the zeroth moment $N(t) = \int n(l,t)dl$, which counts the total number of facets, decreases as $L(t)$ increases. However, its first moment $\int ln(l,t)dl \equiv 1$ is a conserved quantity, reflecting the fact that the conserved quantity in our coarsening faceted surface is the total interface length.

Finally, we presume that under a closure or mean-field hypothesis of statistically independent neighboring facet lengths, it is possible to formulate a probabilistic, length-dependent transport rate

$$v(l,t) \equiv \left\langle \frac{dl_i}{dt} \right\rangle_{\{i|l_i=l\}} \tag{10}$$

describing the average rate of length change for facets of length l at time t.

B. Derivation of an evolution equation

Assuming the existence of $v(l,t)$ implies a population flux $J(l,t)$

$$J(l,t) \equiv n(l,t)v(l,t). \tag{11}$$

For a generic coarsening system, $v(l,t) < 0$ in some neighborhood of $l = 0$; the rate of facet removal is then given by the population flux into the origin

$$R(t) \equiv -J(0,t) > 0. \tag{12}$$

Upon reaching zero length, these facets are removed from the system. However, critically, according to the coarsening rule (6), the two neighboring facets must also be removed and replaced with a new facet having length equal to their sum:

$$(\ldots,\mathcal{L}^-,\mathcal{L},\mathcal{L}^+,\ldots) \xrightarrow{\mathcal{L}\to 0+} (\ldots,\mathcal{L}^- + \mathcal{L}^+,\ldots).$$

Hence, the coarsening process, in addition to transporting facets out of the domain at $l = 0$ at a rate of $R(t)$, induces both a loss $L_C(l,t)$ and a gain $G_C(l,t)$ of facets, which themselves are statistically distributed in length. The shape of these distributions comes from our closure hypothesis, which assumes no correlation between neighboring lengths. Under this hypothesis, the two lost neighbors $\mathcal{L}^-$ and $\mathcal{L}^+$ are each independently distributed according to the probability distribution $\rho(l,t)$. In addition, the facet $\mathcal{L}^- + \mathcal{L}^+$ that replaces them, being the sum of two random variables, must satisfy the joint probability function

$$[\rho * \rho](l,t) = \int_0^l \rho(s,t)\rho(l-s,t)ds. \tag{13}$$

Under these considerations, we therefore have

$$L_C(l,t) = 2R(t)\rho(l,t), \tag{14}$$

$$G_C(l,t) = R(t)[\rho * \rho](l,t), \tag{15}$$

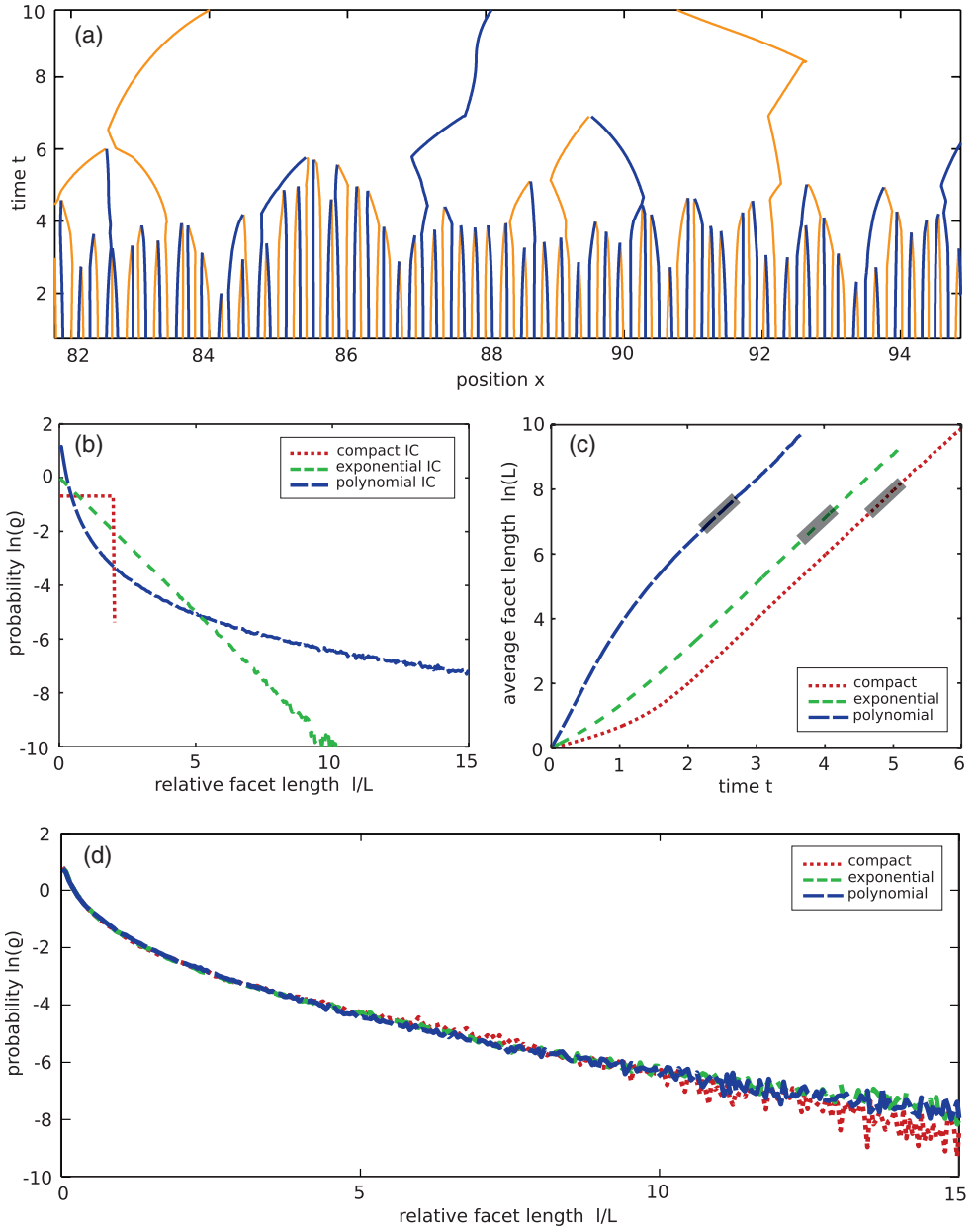

FIG. 2. (Color online) Survey of coarsening behavior. (a) Representative example of the evolution of corners between facets during coarsening (the initial distribution is compact): light (dark) corresponds to hills (valleys), but the problem has up-down symmetry and the distinction is irrelevant. (b) Length distributions for three different initial surfaces, as described by Eqs. (7) (natural log scale). (c) Growth with time of the average facet length $L(t)$ for each of the initial conditions (natural log scale). The scaling state is reached when the curve becomes straight. (d) Numerically observed scaling function $\mathfrak{P}(\frac{l}{L(t)})$ describing the scaling state common to all three of the initial conditions. Each scaling state in (d) was obtained by averaging the data over the corresponding shaded regions in (c).

which are merely the expression within the mean-field framework of the coarsening rule (6). Taken together, the population flux (11), the neighbor-loss rate (14), and the neighbor-replacement rate (15) imply a balance law on the number density given by

$$\frac{\partial n}{\partial t} + \frac{\partial}{\partial l}(nv) = R(\rho * \rho - 2\rho). \tag{16}$$

We now proceed to recast the left-hand side of Eq. (16) purely in terms of the probability density ρ. To that end, it will be useful to introduce the probability flux $\mathcal{J}$,

$$\mathcal{J}(l,t) \equiv \rho(l,t)v(l,t) = \frac{L(t)}{L_0} J(l,t),$$

and the associated probability flux at the origin (rate of flux of probability at 0)

$$\mathcal{R}(t) \equiv \mathcal{J}(0,t) = \frac{L(t)}{L_0} R(t).$$

Noting that integrating the number density (16) with respect to l over the interval $(0,\infty)$ yields a rate of facet loss $\frac{dN}{dt}$ given by

$$\frac{dN}{dt} = \frac{d}{dt}\left(\frac{L_0}{L}\right) = -2R = -2\frac{L_0}{L}\mathcal{R}, \tag{17}$$

we obtain

$$\frac{\partial n}{\partial t} = \frac{\partial}{\partial t}\left(\frac{L_0}{L}\rho\right) = -2\frac{L_0}{L}\mathcal{R}\rho + \frac{L_0}{L}\frac{\partial \rho}{\partial t}. \tag{18}$$

Inserting Eq. (18) into Eq. (16), we conclude that the governing equation for the probability distribution $\rho(l,t)$ is

$$\rho_t + (\rho v)_l = \mathcal{R}(\rho * \rho). \tag{19}$$

This equation, which is our main result, is generic to coarsening faceted surfaces exhibiting binary coarsening, with the effect of the particular facet dynamics limited to the term $v(l,t)$.

C. Predictions: Growth rate and scaling state

To investigate the scaling state of Eqs. (19) and (24), we make the scaling hypothesis that

$$\begin{aligned} \rho(l,t) &= \frac{L_0}{L(t)}\mathcal{P}\left(\frac{l}{L(t)}\right), \\ v(l,t) &= \frac{L(t)}{L_0}\mathcal{V}\left(\frac{l}{L(t)}\right), \end{aligned} \tag{20}$$

where the scaling function $\mathcal{P}$ satisfies

$$\int_0^\infty \mathcal{P}(l)dl = 1, \quad \int_0^\infty l\mathcal{P}(l)dl = 1. \tag{21}$$

This hypothesis leads to two main results. First, we recall that Eq. (17) contained a differential equation on $L(t)$:

$$\begin{aligned} \frac{d}{dt}\left(\frac{L_0}{L}\right) &= -2\mathcal{R}\left(\frac{L_0}{L}\right), \\ \frac{dL}{dt} &= 2\mathcal{R}L. \end{aligned}$$

Under the scaling hypothesis, the probability flux at the origin $\mathcal{R} = -\rho(0,t)v(0,t) = -\mathcal{P}(0)\mathcal{V}(0)$ becomes a constant and so the theory predicts that the average facet length grows according to the exponential relation

$$L(t) = L_0\exp[2\mathcal{R}t]; \tag{22}$$

this form is independent of the particular facet dynamics, which serve only to choose the constants $\mathcal{V}(0)$ and (indirectly) $\mathcal{P}(0)$. Second, upon inserting the ansatz (20) into Eq. (19), we obtain for the scaling function $\mathcal{P}(x)$ the governing equation

$$\begin{aligned} &\frac{d}{dx}[\mathcal{V}(x)\mathcal{P}(x)] \\ &\quad = -\mathcal{V}(0)\mathcal{P}(0)\left\{\int_0^x \mathcal{P}(\xi)\mathcal{P}(x-\xi)d\xi + 2\frac{d}{dx}[x\mathcal{P}(x)]\right\}; \end{aligned} \tag{23}$$

this integro-differential equation implicitly defines $\mathcal{P}(x)$ and can be solved at least numerically. The results (22) and (23) are the central predictions of our theory.

IV. COMPARISON OF THEORY VS DATA FOR OUR EXAMPLE DYNAMICS

We now apply the generic theory of Sec. III to the specific example dynamics (5) from Sec. II and compare the theoretical predictions on ρ with the empirical statistical data ϱ.

A. Application of the general theory

To generate a theory specific to the dynamics (3), all that is required is to calculate the mean-field velocity $v(l,t)$ associated with the dynamics (5) and insert it into the relevant generic equations of Sec. III. From Eq. (5), the application of our neighbor-independent hypothesis leads immediately to

$$v(l,t) = \frac{\mu}{2}[l - L(t)] \quad \text{or} \quad \mathcal{V}(x) = \frac{\mu}{2}(x-1). \tag{24}$$

Inserting Eq. (24) into the generic scaling state equation (23) yields as the definition of the scaling function for this dynamics the equation

$$\begin{aligned} &\frac{d}{dx}[(x-1)\mathcal{P}(x)] \\ &\quad = \mathcal{P}(0)\left\{\int_0^x \mathcal{P}(\xi)\mathcal{P}(x-\xi)d\xi + 2\frac{d}{dx}[x\mathcal{P}(x)]\right\}. \end{aligned} \tag{25}$$

By inspection, a solution to this equation happens to be

$$\mathcal{P}(x) = \exp(-x) \tag{26}$$

and hence the average facet length is predicted to grow at late times as

$$L(t) = e^{-2\mathcal{V}(0)\mathcal{P}(0)t} = e^{\mu\mathcal{P}(0)t} = e^{\mu t}. \tag{27}$$

B. Comparison with data

We now compare the predictions (22) and (26) against steady-state statistics obtained via direct simulation of the dynamics (3), in which we set $\mu = 1$. First, the observed statistical coarsening rate of $e^{1.8t}$, although different from the predicted rate of e^t, is consistent with the generic prediction (22) in that our observed scaling state exhibited $\mathfrak{P}(0) \approx 1.8$. This is unsurprising because the prediction (22) is obtained ultimately from the conservation of total surface length. The discrepancy between actual values is due to a difference in the scaling state itself, shown in Fig. 3. There the predicted exponential distribution is shown in blue; a comparison with the observed distribution (green) reveals qualitative but not quantitative agreement. In particular, although both distributions exhibit exponential decay in the dimensionless relative length l/L, the observed distribution has more of its mass near zero and in the tail, which decays like $\exp(-\frac{x}{2})$ rather than the predicted $\exp(-x)$.

C. Diagnostic tests for the source of disagreement

Seeking the cause of quantitative discrepancies between theory and experiment, we reexamine the two main assumptions used to construct the theory: the existence of a statistical mean field velocity and the noncorrelation of neighboring facet lengths.

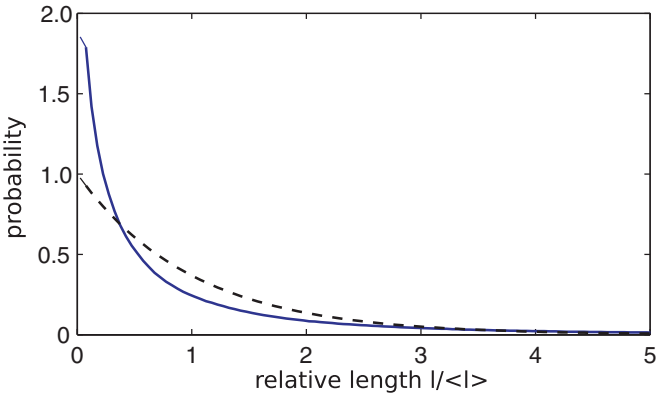

FIG. 3. (Color online) Theory vs simulation. Comparison between the theoretically predicted scaling function $\mathcal{P}(x)$ (solid line) and the empirically observed function $\mathfrak{P}(x)$ (dashed line).

(i) Mean-field velocity. To test the validity of the assumption of an effective flux function $v(l)$, we construct a two-point distribution of length and velocity pairs (l,v) as they occur in the simulated ensembles. A contour plot of the logarithm of this distribution is shown in Fig. 4. Finding the mean velocity for each length gives the statistical v (dashed line), which turns out to compare favorably with the predicted v (solid line). A slight shift between the curves is observed, which we attribute to a discretization error associated with binning our sample data into boxes of width 0.1 in the relative velocity and relative lengths. So this approximation seems to be reasonable.

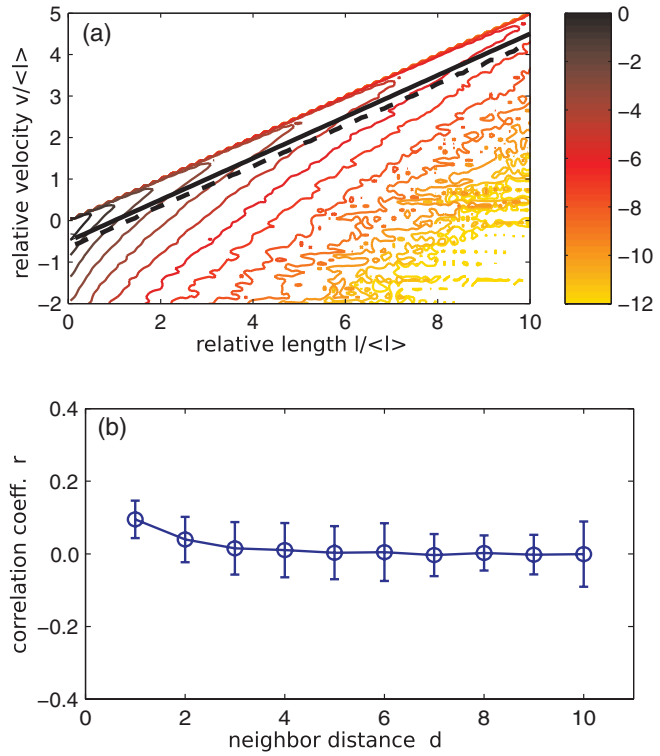

FIG. 4. (Color online) Diagnostic tests. (a) Contour of the logarithm of the steady two-point statistical distribution of dimensionless length-velocity pairs $\ln[\tilde{\varrho}(\frac{l}{L},\frac{v}{L})]$. The mean statistical velocity $\langle \mathfrak{v} \rangle(\frac{l}{L}) = \int_0^\infty s\tilde{\varrho}(\frac{l}{L},s)ds$ is plotted as a dotted line and the predicted velocity $\mathcal{V}(\frac{l}{L})$ is a solid line. (b) Steady-state correlation of facet lengths as a function of neighbor distance d. Plotted is the Pearson product-moment correlation coefficient of all length pairs $(l_i, l_{(i+d)\%n})$, where d is the number of facets between each pair and n is the number of facets in the (periodic) system.

(ii) Noncorrelation. To test the validity of the assumption of noncorrelation between neighboring facets, we measure the correlation coefficient of each nth-neighbor pair for various n. These coefficients tend toward a steady state as the ensembles evolve and that state is shown in Fig. 4(b). There we see a small but possibly significant positive correlation for at least the first two neighbors, suggesting that facets of similar size tend to cluster together: large with large and small with small. Hence the noncorrelation assumption fails, though not spectacularly. This result is not surprising, as the main weakness of the original LSW theory that inspires this work was also a failure to address correlations; later generalizations that corrected this deficiency agreed well with experimental data [41].

V. CONCLUSION

We have presented a mean-field theory for the evolution of length distributions associated with coarsening faceted surfaces. In the spirit of LSW theory, a facet-velocity law governing surface evolution is used to establish a characteristic length-change law; this mean-field velocity, along with a consideration of the effect of binary coarsening events observed during simulation, leads to an continuity equation governing the evolution of the probability distribution. This equation combines a transport term similar to LSW theory with a convolution term reminiscent of coagulation-fragmentation models. However, it is different from either of these in that the latter process occurs at a rate determined by the magnitude of transport at the boundary. Our model therefore serves, apart from the direct application to facet dynamics, as a study of mean-field equations with this structure.

For a sample facet dynamics associated with binary solidification, we find the growth rate, scaling state, and coarsening efficiency predicted by our framework and then compare the predictions to statistics obtained from direct numerical simulation of a large facet ensemble. The results, although not quantitative, agree surprisingly well for a single-point statistic. In addition, the theory captures the essential feature of the dynamically scaling state: a particular mass flux law that drives coarsening by pushing facets away from the average length, moderated by competing terms describing coarsening and continuous rescaling, which push mass toward infinity and zero, respectively. While later improvements to our model addressing neighbor correlation will undoubtedly increase its predictive capabilities, these same forces will still balance in the steady state. The model as presented thus serves as a qualitative explanation of the essential features of the scaling state, as well as a guide to further research efforts.

ACKNOWLEDGMENT

S.A.N. was supported by NASA Graduate Student Researchers Program No. NGT5-50434 for the early stages of this work.

[1] A. N. Kolmogorov, Dokl. Akad. Nauk SSSR **65**, 681 (1940).
[2] A. van der Drift, Philips Res. Rep. **22**, 267 (1967).
[3] M. E. Gurtin and P. W. Voorhees, Acta Mater. **46**, 2103 (1998).
[4] S. J. Watson and S. A. Norris, Phys. Rev. Lett. **96**, 176103 (2006).
[5] L. Pfeiffer, S. Paine, G. H. Gilmer, W. van Saarloos, and K. W. West, Phys. Rev. Lett. **54**, 1944 (1985).
[6] D. K. Shangguan and J. D. Hunt, J. Cryst. Growth **96**, 856 (1989).
[7] C. L. Emmot and A. J. Bray, Phys. Rev. E **54**, 4568 (1996).
[8] S. J. Watson, F. Otto, B. Y. Rubinstein, and S. H. Davis, Physica D **178**, 127 (2003).
[9] S. A. Norris, S. H. Davis, P. W. Voorhees, and S. J. Watson, J. Cryst. Growth **310**, 414 (2008).
[10] C. Wild, N. Herres, and P. Koidl, J. Appl. Phys. **68**, 973 (1990).
[11] J. M. Thijssen, H. J. F. Knops, and A. J. Dammers, Phys. Rev. B **45**, 8650 (1992).
[12] Paritosh, D. J. Srolovitz, C. C. Battaile, and J. E. Butler, Acta Mater. **47**, 2269 (1999).
[13] J. Zhang and J. B. Adams, Modell. Simul. Mater. Sci. Eng. **10**, 381 (2002).
[14] J. Zhang and J. B. Adams, Comput. Mater. Sci. **31**, 317 (2004).
[15] J. M. Thijssen, Phys. Rev. B **51**, 1985 (1995).
[16] S. Barrat, P. Pigeat, and E. Bauer-Grosse, Diam. Relat. Mater. **5**, 276 (1996).
[17] G. Russo and P. Smereka, SIAM J. Sci. Comput. **21**, 2073 (2000).
[18] P. Smereka, X. Li, G. Russo, and D. J. Srolovitz, Acta Mater. **53**, 1191 (2005).
[19] S. A. Norris and S. J. Watson, Acta Mater. **55**, 6444 (2007).
[20] W. Ostwald, Z. Phys. Chem. **34**, 495 (1900).
[21] W. W. Mullins, Philos. Mag. **6**, 1313 (1961).
[22] N. Cabrera, in *Symposium on Properties of Surfaces*, ASTM Materials Science Series—4 (American Society for Testing and Materials, Philadelphia, 1963).
[23] J. W. Cahn and J. E. Hilliard, J. Chem. Phys. **28**, 258 (1958).
[24] F. Liu and H. Metiu, Phys. Rev. B **48**, 5808 (1993).
[25] A. A. Golovin, S. H. Davis, and A. A. Nepomnyashchy, Physica D **122**, 202 (1998).
[26] J. Stavans, Rep. Prog. Phys. **56**, 733 (1993).
[27] V. E. Fradkov and D. Udler, Adv. Phys. **43**, 739 (1994).
[28] H. J. Frost and C. V. Thompson, Curr. Opin. Solid State Mater. Sci. **1**, 361 (1996).
[29] C. V. Thompson, Solid State Phys. **55**, 269 (2001).
[30] G. Schliecker, Adv. Phys. **51**, 1319 (2002).
[31] T. P. Schulze and R. V. Kohn, Physica D **132**, 520 (1999).
[32] I. M. Lifshitz and V. V. Slezov, Sov. Phys. JETP **38**, 331 (1959).
[33] I. M Lifshitz and V. V. Slyozov, J. Phys. Chem. Solids **19**, 35 (1961).
[34] C. Wagner, Z. Elektrochem. **65**, 581 (1961).
[35] C. W. J. Beenakker, Phys. Rev. Lett. **57**, 2454 (1986).
[36] H. Flyvbjerg, Phys. Rev. E **47**, 4037 (1993).
[37] K. Barmak, E. Eggeling, M. Emelianenko, Y. Epshteyn, D. Kinderlehrer, R. Sharp, and S. Ta'asan, Discrete Cont. Dyn. Syst. Ser. A **30**, 427 (2011).
[38] M. von Smoluchowski, Phys. Z. **17**, 557 (1916).
[39] T. E. W. Schumann, Q. J. R. Meteorol. Soc. **66**, 195 (1940).
[40] G. Menon, B. Niethammer, and R. L. Pego, Trans. Am. Math. Soc. **362**, 6591 (2010).
[41] M. Marder, Phys. Rev. A **36**, 858 (1987).